1656–1670 *Nucleic Acids Research, 2014, Vol. 42, No. 3* *Published online 14 November 2013*
doi:10.1093/nar/gkt1134

RNA-dependent dynamic histone acetylation regulates *MCL1* alternative splicing

Dilshad H. Khan[1], Carolina Gonzalez[1], Charlton Cooper[2], Jian-Min Sun[2], Hou Yu Chen[2], Shannon Healy[1], Wayne Xu[1], Karen T. Smith[3], Jerry L. Workman[3], Etienne Leygue[2] and James R. Davie[1,2,*]

[1]Department of Biochemistry and Medical Genetics, University of Manitoba, Manitoba Institute of Child Health, Winnipeg, Manitoba, R3E 3P4, Canada, [2]Department of Biochemistry and Medical Genetics, University of Manitoba, Manitoba Institute of Cell Biology, Winnipeg, Manitoba, R3E0V9, Canada and [3]Stowers Institute for Medical Research, Kansas City, Missouri 64110, USA

Received July 3, 2013; Revised October 8, 2013; Accepted October 23, 2013

ABSTRACT

Histone deacetylases (HDACs) and lysine acetyltransferases (KATs) catalyze dynamic histone acetylation at regulatory and coding regions of transcribed genes. Highly phosphorylated HDAC2 is recruited within corepressor complexes to regulatory regions, while the nonphosphorylated form is associated with the gene body. In this study, we characterized the nonphosphorylated HDAC2 complexes recruited to the transcribed gene body and explored the function of HDAC-complex-mediated dynamic histone acetylation. HDAC1 and 2 were coimmunoprecipitated with several splicing factors, including serine/arginine-rich splicing factor 1 (SRSF1) which has roles in alternative splicing. The co-chromatin immunoprecipitation of HDAC1/2 and SRSF1 to the gene body was RNA-dependent. Inhibition of HDAC activity and knockdown of HDAC1, HDAC2 or SRSF1 showed that these proteins were involved in alternative splicing of *MCL1*. HDAC1/2 and KAT2B were associated with nascent pre-mRNA in general and with *MCL1* pre-mRNA specifically. Inhibition of HDAC activity increased the occupancy of KAT2B and acetylation of H3 and H4 of the H3K4 methylated alternative *MCL1* exon 2 nucleosome. Thus, nonphosphorylated HDAC1/2 is recruited to pre-mRNA by splicing factors to act at the RNA level with KAT2B and other KATs to catalyze dynamic histone acetylation of the *MCL1* alternative exon and alter the splicing of *MCL1* pre-mRNA.

INTRODUCTION

Lysine acetyltransferases (KATs) and histone deacetylases (HDACs) catalyze dynamic acetylation of proteins, including histones, associated with transcribed DNA (1–7). KATs often have transcriptional coactivator activity, increasing the level of acetylated histones and enhancing transcription when recruited to a gene promoter by a transcription factor (1,8–10). HDAC1 and HDAC2 are present in multiprotein corepressor complexes (Sin3, NuRD, CoREST), which are recruited to regulatory regions by transcription factors (11,12). Phosphorylation of HDAC1 (at S393/421/S423) and HDAC2 (at S394/422/S424) is required for the formation of these corepressor complexes, which are recruited to the regulatory regions of transcribed genes (11–14). In contrast, the nonphosphorylated HDAC2 is associated with the body of transcribed genes (12). Although the unmodified HDAC2 is more abundant than highly phosphorylated HDAC2, it is the highly phosphorylated form that is preferentially crosslinked to chromatin with formaldehyde or cisplatin (11). However, through the use of a dual crosslinking chromatin immunoprecipitation (ChIP) assay, all isoforms of HDAC1 and HDAC2 could be mapped along regulatory and coding regions of transcribed genes, with the unmodified HDAC2 being associated with the coding region (12,15). Yet, it remains to be determined which proteins the unmodified (nonphosphorylated) HDAC1 and HDAC2 interact with when targeted to the body of transcribed genes.

Recent studies suggest a role for HDAC1 and HDAC2 in alternative splicing (16,17). Approximately 95% of human multiexon genes generate alternatively spliced transcripts, giving rise to mature mRNA isoforms coding for functionally different proteins. Most of these splicing events are regulated in a tissue- and/or developmental stage-specific manner or in response to naturally

*To whom correspondence should be addressed. Tel: +1 204 975 7732; Fax: +1 204 977 5691; Email: davie@cc.umanitoba.ca

occurring external stimuli (18–20). Pre-mRNA splicing is a cotranscriptional process, which is regulated by RNA polymerase II (RNAPII) elongation rate, as inclusion of an alternative exon occurs only if splicing components have time to interact with the nascent RNA before its 3′-end cleavage and release (21–25).

There is emerging evidence that histone modifications and chromatin structure influence splicing, and vice-versa pre-mRNA splicing itself influences chromatin organization (23–30). Several studies have suggested or demonstrated a correlation between local increase in histone acetylation and exon skipping; however, the mechanisms involved are poorly understood (16,17,29,31). The skipping of NCAM exon 18 upon membrane depolarization of neuronal cells was linked to localized increased histone H3 acetylation (H3K9ac) and could be replicated by the HDAC inhibitor trichostatin A (TSA) (29). In HeLa cells treated with the pan-HDAC inhibitor, sodium butyrate, splicing-sensitive exon-arrays detected a change in the splicing pattern of ~700 genes (16). The levels of serine/arginine-rich (SR) proteins and other proteins involved in splicing, as well as the acetylation status of splicing factors were not altered by 15 h of HDAC inhibition. In the case of the fibronectin (*FN1*) alternative exon 25 (also named EDB), histone H4 acetylation increased rapidly following HDAC inhibition and reached its maximal level after 6–9 h. An increased exclusion of exon 25 could be detected within this time frame, if cells were treated with 5,6-dichloro-1-β-D-ribobenzimidazole (DRB), a reversible inhibitor of RNAPII, such that analysis would be limited to *de novo* synthesized pre-mRNA (16). It was shown that HDAC inhibition decreased the association of one of the SR proteins, SRSF5 (also known as SRp40) with the *FN1* gene, including but not restricted to exon 25. siRNA-mediated knockdown of HDAC1, but not HDAC2, resulted in exon 25 skipping, suggesting that HDAC1 is primarily involved in the splicing regulation of this gene (16), but the mode of action of HDAC1 remains unclear. In neuronal cells, it was suggested that HDAC2 association with the splicing regulator Hu proteins enhanced the localized histone acetylation at the alternative exons of *NF1* and *FAS* genes, an event that was correlated with a localized increased elongation rate and the exclusion of these exons. *In vitro*, the HuR proteins inhibited HDAC2 activity (17). It was proposed that HuR proteins, cotranscriptionally recruited to their target RNA sequences, inhibit HDAC2 activity through a 'reach back' interaction with chromatin (17). However, the association of HDAC2 with the alternative exons of *NF1* and *FAS* genes was not directly demonstrated. Thus, a correlation between histone acetylation and skipping of alternative exons was observed, but the recruitment and distribution along the body of the transcribed genes of HDACs and KATs, the enzymes catalyzing histone acetylation, were not addressed in these studies.

In this study, we demonstrate that the serine/arginine-rich splicing factor 1 (SRSF1, also known as ASF/SF2) coimmunoprecipitated with HDAC1 and nonphosphorylated HDAC2. Since this is a SR protein with a major role in alternative splicing (32), we explored the role of HDAC1 and HDAC2 in splicing using the human myeloid cell leukemia sequence 1 (*MCL1*) gene as a model gene. The *MCL1* gene undergoes alternative splicing of exon 2 and produces a protein that either prevents or supports cell death depending on the splice isoform. The long form MCL1L is an anti-apoptotic protein, while the short form MCL1S is pro-apoptotic (33). We have analyzed the effects of HDAC pan- and Class I specific inhibitors on the splicing of the *MCL1* gene. We show that HDAC inhibitors enhanced histone acetylation over exon 2, an event that paralleled exon 2 exclusion. We also show, for the first time, that HDAC1 and HDAC2 are recruited to the *MCL1* pre-mRNA to catalyze, in concert with KATs, dynamic histone acetylation of the exon 2 nucleosome.

MATERIALS AND METHODS

Cell cultures and treatments

HEK293, Flp-In 293 stable cells expressing HDAC2-WT -V5 or HDAC2-3S/A-V5 and MCF7 cells were cultured in Dulbecco's modified Eagle's media (Gibco), and HCT116 cells were cultured in McCoy's 5A media (Sigma), supplemented with 10% fetal bovine serum (FBS), 100 units/ml penicillin, 100 μg/ml streptomycin, and 250 ng/ml amphotericin B, and were maintained at 37°C in a humidified atmosphere containing 5% CO_2. Cells were treated with HDAC inhibitors, TSA (250 nM) (Sigma), apicidin (150 nM) (Sigma) or butyrate (2 mM) (Sigma) for indicated time periods. When indicated, subconfluent cells (~80–90%) were serum-starved for 48 h and then either left untreated or treated with TPA (12-*O*-tetradecanoylphorbol-13-acetate) (100 nM, Sigma) for 30 or 60 min. In inhibition studies, serum starved cells were pretreated with either TSA or apicidin for 30 min followed by treatment with phorbol ester, TPA (0, 30 or 60 min).

Mass spectrometry

HDAC1 or HDAC2 complexes were immunoprecipitated from HEK293 cells or Flp In 293 stable cells expressing WT-HDAC2-V5 or HDAC2-3S/A-V5, with anti-HDAC1, anti-HDAC2 (Affinity BioReagents) or anti-V5 (Abcam) antibodies. When mentioned, nuclear extracts from Flp In 293 stable cells expressing WT-HDAC2-V5 or HDAC2-3S/A-V5 were treated with RNase A (5 μg of RNase A for 20 min at 37°C) prior to immunoprecipitation with anti-V5 antibodies. Covalent immobilization of the antibodies onto the surface of Dynabeads® Protein G (Invitrogen) was used for coimmunoprecipitation of intact protein complexes. The immunoprecipitated fractions were eluted from the Dynabeads with 1% SDS/0.1 M $NaHCO_3$. The eluted fractions were vacuum dried and washed with 100 mM NH_4HCO_3 and iodoacetamide. After lyophilization, the fractions were digested with trypsin for 16 h at 37°C. The nano-liquid chromatography and tandem mass spectrometry were performed on the trypsin-digested samples as described previously (34). The MSDB, version 20060831, database was searched using the Global Proteome Machine (http://www.thegpm.org) search engine to identify the peptide sequences.

Immunoprecipitation and immunoblotting

Cells were harvested and lysed in cold lysis buffer (50 mM Tris–HCl, pH 8.0, 150 mM NaCl, 1 mM EDTA, 0.5% NP-40) containing phosphatase and protease inhibitors (Roche), and immunoprecipitations were done as described earlier (11). In brief, 500 µg total cellular or nuclear extracts were incubated with 3.0 µg of anti-HDAC1 (Affinity Bioreagents), anti-HDAC2 (Affinity Bioreagents), anti-SRSF1 (Santa Cruz Biotechnology), anti-acetyl lysine (Cell Signaling Technology), anti-H3 (Millipore) or anti-RNAPIIS2ph (Abcam) antibodies overnight at 4°C. An amount of 40 µl of protein A/G UltraLink resin (Pierce) were added and incubated for 3 h at 4°C. The beads were then washed four times with ice-cold lysis buffer. Immunoprecipitation with isotype specific nonrelated IgG was performed as negative control. One-third of the fractions immunoprecipitated by anti-HDAC1 or anti-HDAC2 antibodies and one-half of the fractions immunoprecipitated by anti-RNAPIIS2ph or anti-SRSF1 antibodies were analyzed by immunoblotting, while equivalent volumes of lysate (Input) and immunodepleted fractions were analyzed, corresponding to 20 (for anti-HDAC1 or anti-HDAC2 antibodies) or 25 µg (for anti-RNAPIIS2ph or anti-SRSF1 antibodies) of lysate proteins. When mentioned, cellular extracts were treated with RNase A (400 µg/ml of RNase A for 30 min at 37°C) before immunoprecipitation reaction. Immunochemical staining was performed with rabbit polyclonal antibodies against human HDAC1 (Affinity BioReagents), HDAC2 (Affinity BioReagents), HDAC2 (phospho S394) (Abcam), SIN3A (Affinity BioReagents), RCOR1 (Abcam) or mouse monoclonal antibodies against HDAC2 (Millipore) or RBPP4 (Abcam).

HDAC activity assay

HDAC activity assay was performed with the Fluor-de-Lys® HDAC fluorometric activity assay kit (Enzo life sciences) following the manufacturer's instructions. SRSF1 complex was immunoprecipitated from 500 µg of HCT116 cell lysates with 5 µg of mouse monoclonal anti-SRSF1 antibody (Santa Cruz Biotechnology). As a negative control, immunoprecipitation with isotype-specific nonrelated IgG was performed. An amount of 40 µl of protein A/G UltraLink resin (Pierce) were added and incubated for 3 h at 4°C. The beads were washed three times with IP buffer (50 mM Tris–Cl pH 8.0, 150 mM NaCl, 1 mM EDTA, 0.5% NP-40) and twice with the HDAC activity assay buffer before used for the HDAC activity assay. For the assay, the beads treated or not with 1.0 µM TSA were incubated with 150 µM Fluor de Lys® Substrate for 30 min at room temperature with rocking. After that, the developer I solution containing 1.0 µM TSA was added and aliquots were incubated for another 30 min to stop the reactions. For boiling control, after immunoprecipitation, the beads were boiled for 15 min and the assay was performed as mentioned above. The fluorescence signal was measured using fluorometric plate reader (Spectra MAX GEMINI XS, Molecular devices).

ChIP and re-ChIP assays

ChIP and re-ChIP experiments were done as previously described with an additional protein–protein crosslinking step with DSP (dithiobis[succinimidylpropionate]) (Thermo Fisher Scientific) (35). Cells were incubated with 1.0 mM DSP for 30 min at room temperature according to manufacturer's instruction (Pierce), followed by crosslinking with formaldehyde for 10 min. Dual crosslinked chromatin was processed to mononucleosomes by micrococcal nuclease (MNase) (Worthington Biochemical Corporation) digestion (2.5 U of MNase/A_{260} of nuclear suspension) for 40 min at 37°C (35). ChIPs were done with anti-RNAPIIS2ph (Abcam), anti-HDAC2 (Affinity Bioreagents), anti-SRSF1 (Santa Cruz Biotechnology), anti-H3K14ac (Abcam), anti-H3K9ac (Abcam), anti-acH3 (Millipore), anti-H4K5ac (Millipore), anti-H4K8ac (Millipore), anti-acH4 (Millipore), anti-H3 (Millipore), anti-KAT2B (Abcam) or anti-KAT7 (Santa Cruz Biotechnology) antibodies. Negative control included performing ChIP/reChIP assays with an isotype matched nonrelated IgG. For RNase A-treated extracts, DSP and formaldehyde crosslinked chromatin was processed to mononucleosomes and treated with 400 µg/ml of RNase A for 30 min at 37°C. The further processing of chromatin fragments were performed as previously described (35). Input and ChIP/reChIP DNAs were quantified using PicoGreen assay. Equal amounts of input and immunoprecipitated DNA (1.0 ng) or re-ChIP (0.5 ng) DNA were used to perform SYBR Green real-time PCR on iCycler IQ5 (BioRad). Primers are described in Supplementary Table S1. Enrichment values, calculated as previously described (35), are relative to input DNA and are the mean of three independent experiments. The error bars indicate standard deviation ($n = 3$).

ChIP DNA library, sequencing and ChIPSeq data analysis

ChIPSeq libraries for H3K4me3 antibody (Abcam) were prepared according to the 5500 SOLiD fragment library protocol (Life technologies). Briefly, a quantity of 18 ng of ChIP DNA was end-repaired and size selected (100–250 bp), followed by dA tailing, ligation of SOLiD barcodes and library PCR amplification. Libraries were subjected to emulsion PCR (ePCR) and loaded on the flowchip for sequencing. Total 18 369 095 and 30 049 407 50-base SOLiD sequence reads were generated from H3K4me3 ChIP sample and input sample, respectively. The sequence reads were mapped on human genome reference hg19 using LifeScope Genomic Analysis Software v2.5.1 (Life Technologies) with 2-mismatch setting and the best score mapping when multiple mapping occurs. The mapping quality was inspected using the Bamstats module. More than 83% of reads were mapped. The H3K4me3 marker peaks were called using MACS package (36) and annotated using CEAS program (37). The H3K4me3 signals along the *MCL1* gene were viewed by the Partek Genomic Suite (Partek Inc. St. Louis, USA).

siRNA-mediated transient knockdown

HCT116 cells were transfected at ~30–40% confluency with 75 nM of scramble (Nontargeting Pool), human HDAC1, HDAC2 or SF2 (SRSF1) ON-TARGET plus SMARTpool siRNAs (Thermo Scientific-Dharmacon), using Polyplus Interferin siRNA transfection reagent (VWR) according to manufacturer's protocol. Forty-eight hours after transfections, cells were harvested and the knockdown efficiencies were analyzed by immunoblotting and changes in *MCL1* splicing were analyzed by radiolabeled PCR (^{32}P). For ChIP assays, cells were dual crosslinked after the transfection period and processed as described above.

RNA isolation, reverse transcription PCR and radiolabeled- PCR (^{32}P)

Total RNA was isolated from untreated and treated HCT116 cells using RNeasy Plus Mini Kit (Qiagen) according to manufacturer's instructions. Total RNA (400 ng) was used as template for synthesis of cDNA using M-MLV reverse transcriptase and Oligo dT primers (Invitrogen). Radiolabeled ^{32}P PCR was performed in a final volume of 15 µl containing 7.5 ng of cDNA, in the presence of 1× PCR buffer (Invitrogen), 1.5 mM $MgCl_2$, 0.2 mM dNTPs, 0.2 µM of each primer, 1 unit of Platinum Taq DNA polymerase and 10 nM α^{32}P dCTP (10 mCi/ml). *MCL1* PCR conditions comprised a 5-min incubation at 95°C, followed by 35 cycles of (95°C for 30 s, 56°C for 45 s, 72°C for 45 s) and a final incubation at 72°C for 10 min. Primers are described in Supplementary Table S1. Following PCR amplification, 2.5 µl of radiolabeled PCR products were denatured in 80% formamide buffer (containing 1 mM EDTA pH 7.5, 0.1% xylene xyanol, 0.1% bromophenol blue) and run on a denaturing polyacrylamide gel (6%) at 40 W (constant wattage). After electrophoresis, the gels were dried and exposed to a Molecular Imager TM FX (BioRad, Hercules, and CA) and PCR signals were quantified. Percentages of the short isoform (*MCL1S*) among total transcripts are presented as percentages of exon 2 exclusion. The student's *t*-test for paired samples was used for calculation of statistical significance.

RNA-CLIP assay (crosslinking and immunoprecipitation of RNA–protein complexes)

Cycling HCT116 cells, treated or not with HDAC inhibitors TSA (250 nM) or apicidin (150 nM) for 2 h, were either incubated with 1.0 mM DSP for 30 min or not, followed by irradiation under ultraviolet (UV) light (400 mJ/cm^2) (Stratalinker). Cells were harvested and lysed in ice-cold lysis buffer [20 mM Tris–HCl at pH 7.5, 100 mM NaCl, 10 mM $MgCl_2$, 0.5% NP-40, 0.5% Triton X100, 0.1% SDS, protease and phosphatase inhibitor cocktail (Roche), 80 U/ml RNasin (Promega)] with sonication. The cellular extracts were treated with a dilute cocktail of RNase A/T1 (Ambion) as previously described (32). Cellular extracts were precleared with protein A/G UltraLink resin (Pierce) and tRNA at 100 µg/ml for 2 h at 4°C. The lysate was incubated with anti-HDAC1, anti-HDAC2, anti-SRSF1 or anti-KAT2B antibodies or normal rabbit or mouse IgG on a rotator overnight at 4°C, followed by addition of protein A/G UltraLink resin (Pierce) for 3 h at 4°C. Beads were then washed six times using the lysis buffer. The beads were resuspended in 200 µl of lysis buffer and then treated with proteinase K (2 mg/ml) for 1 h at 55°C. Immunoprecipitated RNA was then extracted using Trizol (Invitrogen) and precipitated with ethanol. RNA precipitates were resuspended in 20 µl of ultrapure water, treated with RQ DNase (Promega) for 1 h at 37°C. Equal amounts of input and immunoprecipitated RNA were used for cDNA synthesis and reversed transcribed using random oligo dT and random hexamers with SuperScript III reverse transcriptase (Invitrogen) following the manufacturer's specifications. The resulting cDNA was analyzed by real-time PCR with the indicated primer sets in Supplementary Table S1. Results are representative of three independently performed experiments.

RESULTS

HDAC1 and HDAC2 interact with splicing factors in a RNA-independent manner

To identify the proteins associated with HDAC1 and HDAC2, we established Flp-In 293 stable cell lines expressing V5-tagged versions of wild type HDAC2 (WT) or a triple mutant HDAC2 (3S/A), which has the three CK2 phosphorylation sites mutated from serine to alanine (S/A mutation at S394, 422, 424), and immunoprecipitated the HDAC complexes using antibodies against the V5 tag (38). We also isolated native HDAC1/2 complexes from HEK293 cells. Proteins coimmunoprecipitated with the HDACs were identified by mass spectrometry. Table 1 shows that HDAC1 and HDAC2 were bound to the Sin3, NuRD and CoREST complexes as well as to numerous RNA splicing proteins. Nonphosphorylated HDAC2, however, interacted with RNA splicing factors, but not with components of corepressor complexes, confirming previous results that HDAC2 phosphorylation is required for corepressor complex formation (11–13). Since HDAC1 and HDAC2 were associated with splicing factors, we determined whether these interactions were mediated by RNA. Nuclear extracts from Flp-In 293 expressing HDAC2-WT-V5 or HDAC2-3S/A-V5 were treated with RNase A prior to immunoprecipitation with anti-V5 antibodies. The RNase A treatment did not affect the association of HDAC2 with RNA splicing factors, showing that the interactions between these proteins were RNA-independent (Supplementary Table S2).

Among the RNA-binding proteins associated with HDAC1 and HDAC2, we focused our studies on SRSF1, which was reproducibly detected in the mass spectrometry analyses. SRSF1 is a sequence-specific RNA-binding factor that promotes spliceosome formation by binding to exonic splicing enhancers during pre-mRNA splicing (39). Interactions between HDAC1 or HDAC2 and SRSF1 were validated in reciprocal coimmunoprecipitation assays using HCT116 cell lysates

Table 1. Proteins associated with exogenous wild-type or mutated (3S/A) HDAC2, and with endogenous HDAC1 and HDAC2

	Flp-In 293 expressing HDAC2-WT-V5 Anti-V5 IP	Flp-In 293 expressing HDAC2-3S/A-V5 Anti-V5 IP	HEK293 Anti-HDAC2 IP	HEK293 Anti-HDAC1 IP
Corepressor complexes	HDAC1, 2	HDAC1, 2	HDAC1, 2	HDAC1, 2
	RBBP4, 6, 7		RBBP4, 6, 7	RBBP4, 6, 7
	MTA1, 2, 3		MTA1, 2, 3	MTA1, 2, 3
	SIN3A		SIN3A	SIN3A
	CHD3, 4		CHD3, 4	CHD3, 4
	MBD2, 3		MBD2, 3	MBD2
	RCOR1		RCOR1	RCOR1
	KDM1A		KDM1A	KDM1A
RNA splicing	SRSF1, 3, 4, 6, 7, 10, 11, 12	SRSF1, 3, 4, 6, 7, 10, 11, 12	SRSF1, 4, 6, 7, 11, 12	SRSF1, 3, 4, 6, 7, 11, 12
	HNRNPA2/B1, H, K, M, Q, U	HNRNPA2/B1, H, K, M, Q, U	HNRNPA2/B1, H, K, M, Q, U	HNRNPA2/B1, H, K, L, M, Q, U
	RBMX	RBMX	RBMX	RBMX
	PTBP1	PTBP1	PTBP1	PTBP1
	SNRNP200	SNRNP200	SNRNP200	SNRNP200
	SNRNP40	SNRNP40	SNRNP40	SNRNP40
	SNRPB2	SNRPB2	SNRPB2	SNRPB2
	SNRPD1	SNRPD1	SNRPD1	SNRPD1
	SNRPD3	SNRPD3	SNRPD3	SNRPD3
	SNRPE	SNRPE	SNRPE	SNRPE
	PRPF4B, 6, 8, 19	PRPF4B, 6, 8, 19	PRPF4B, 6, 8, 19	PRPF4B, 6, 8, 19
	RBM22, 25, 39	RBM22, 25, 39	RBM22, 25, 39	RBM22, 25, 39
	SF3B1- 4	SF3B1- 4, SF3A1, 2	SF3B2	SF3B1,3
	SFPQ	SFPQ		

Except for HNRNPQ, which is coded for by *SYNCRIP* gene, immunoprecipitated proteins are identified by the genes encoding them.

(Figure 1A). SRSF1 coimmunoprecipitated with HDAC2, but not with either the serine 394 phosphorylated form of HDAC2 (HDAC2-S394ph) or the SIN3A, RBPP4 or RCOR1 (also known as CoREST), components of corepressor complexes (Figure 1A). Thus, the data suggest that HDAC2 phosphorylation specifies its incorporation into corepressor complexes at upstream promoter elements of genes, while lack of phosphorylation directs HDAC2 association with complexes involved in pre-mRNA splicing. Similarly, SRSF1 coimmunoprecipitated with unmodified HDAC2, but not with HDAC2-S394ph in MCF7 and HEK293 cells (Supplementary Figure S1).

As splicing regulator HuR proteins interact with HDAC2 and inhibit its activity (17), we measured the HDAC activity in the SRSF1 immunoprecipitate. Figure 1B shows that the HCT116 cell lysate fraction immunoprecipitated by antibodies against SRSF1 had HDAC activity, which was sensitive to the HDAC inhibitor TSA or to heat inactivation. Furthermore, the addition of a recombinant GST-SRSF1 fusion protein to HDAC2 complexes immunoprecipitated from a HCT116 cell lysate with antibodies against HDAC2 did not affect HDAC activity (data not shown). Thus, SRSF1 did not inhibit HDAC activity.

HDAC1 and HDAC2 co-chromatin immunoprecipitate with SRSF1 along the body of transcribed genes

Following transcription initiation, RNAPII pauses until it becomes elongation-competent when its CTD is phosphorylated at serine 2 (RNAPIIS2ph). SRSF1 is recruited to RNAPIIS2ph, as soon as the transition to productive elongation occurs (40). In agreement with this result, SRSF1 was shown to accumulate along the body of the *FOS* gene only upon induction (41). Similarly, we found that SRSF1, HDAC1 and HDAC2 were recruited to the body of the *FOSL1*, *MCL1* (Supplementary Figure S2) and *TFF1* (data not shown) genes upon induction. To determine if HDAC1 and HDAC2 are co-chromatin immunoprecipitated with SRSF1 to the body of transcribed genes, we studied three different genes in two cell lines. Serum-starved HCT116 cells were stimulated with the phorbol ester, TPA, to activate the MAPK pathway and induce the expression of immediate-early genes (i.e. *FOSL1*) (35). To determine the co-occupancy of HDAC2/SRSF1 or HDAC1/SRSF1 on *FOSL1* exons 1 and 4, sequential ChIP assays were performed, using the dual crosslinking high resolution ChIP assay sequentially with antibodies against HDAC2 or HDAC1 and SRSF1. Prior to TPA induction, there was no HDAC2/SRSF1 or HDAC1/SRSF1 associated with these exons, but following TPA induction, HDAC2/SRSF1 or HDAC1/SRSF1 loaded onto the *FOSL1* gene (Figure 1C and Supplementary Figure S3A). The expression of the *MCL1* gene is also increased in response to the MAPK pathway activation (42). Accordingly, we observed an increased HDAC2 or HDAC1 and SRSF1 co-occupancy on *MCL1* exons 1 and 3, upon TPA induction (Figures 1D and Supplementary Figure S3A). Likewise, induction of the *TFF1* gene in MCF7 cells by either estrogen or TPA (43,44) resulted in the co-occupancy of HDAC2 and SRSF1 along the body of the gene (Supplementary Figure S3C). Thus, the co-occupancy of HDAC1 or HDAC2 and SRSF1 along the body of transcribed genes was RNA-dependent, and occurred

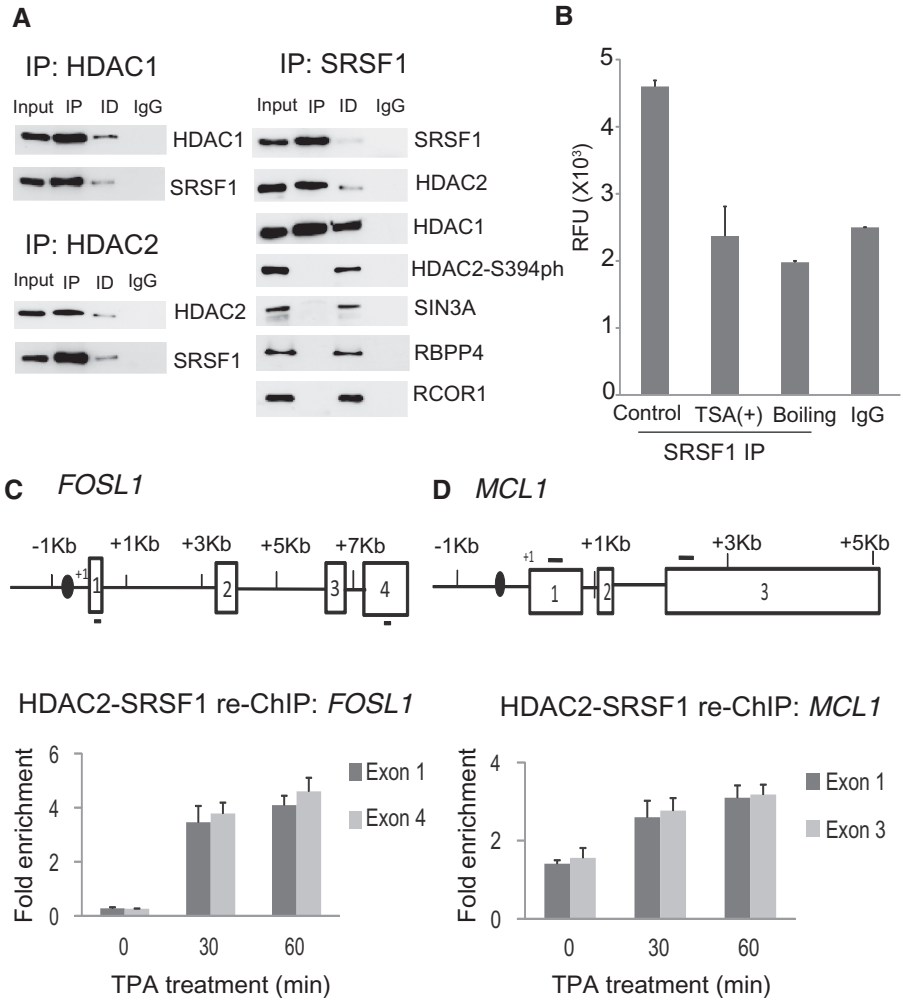

Figure 1. SRSF1 coimmunoprecipitate with HDAC1 and HDAC2, but not with HDAC2-S394ph, along the body of transcribed genes. (**A**) HCT116 cell lysates (500 µg) were incubated with anti-HDAC1, anti-HDAC2 or anti-SRSF1 antibodies. Immunoprecipitated (IP) and immunodepleted (ID) fractions were analyzed by immunoblot assay for the presence of indicated proteins, as described in 'Materials and Methods' section. Isotype specific nonrelated IgGs were used as negative control. (**B**) HDAC activity in anti-SRSF1 immunoprecipitate from HCT116 cell lysate was measured, using a fluorometric activity assay. RFU indicates relative fluorescent units. (**C**) Schematic representation of *FOSL1* gene, with amplicons generated in ChIP assays shown below map. Open boxes represent exons, and oval represents the upstream promoter element. HDAC2/SRSF1 re-ChIP experiments were performed on DSP- and formaldehyde-crosslinked mononucleosomes prepared from serum-starved HCT116 cells treated with 100 nM TPA for 0, 30 or 60 min. (**D**) As in (C), for *MCL1* gene.

whether splicing was constitutive (*FOSL1* and *TFF1*) or alternative (*MCL1*).

SRSF1, HDAC1 and HDAC2 regulate alternative splicing of *MCL1* RNA

SRSF1 regulates the alternative splicing of many genes (32), including the splicing of *MCL1* pre-mRNA, which undergoes alternative splicing of exon 2 (45) (Figure 2A). Hence, toward the understanding of the mechanisms by which HDAC inhibitors alter pre-mRNA splicing, we selected *MCL1* as a model gene. It has been previously shown that a decline in availability of SRSF1 favored the production of the pro-apoptotic *MCL1* short form (*MCL1S*) transcript (exclusion of exon 2) (45). Similarly we found that knockdown of SRSF1 affected the splicing of *MCL1* transcripts in HCT116 cells (Figure 2B). We observed a greater exclusion of alternative exon 2 in HCT116 cycling cells transiently transfected with SRSF1 siRNA compared to cells transfected with scramble (nontargeting) siRNA. Four independent sets of data showed that the increase of the percentage of *MCL1* exon 2 exclusion (*MCL1S* transcripts) in SRSF1 knockdown cells had a strong statistical significance (Figure 2B). A value of 84.5 ± 5.3% SRSF1 knockdown was determined by immunoblot analysis (Supplementary Figure S4A).

Next, we determined the effect of HDAC inhibition on the alternative splicing of *MCL1*. To control for any off-target effect, we used two HDAC inhibitors with different selectivities: TSA or apicidin. TSA is considered a pan-inhibitor; meaning it inhibits Class I and IIb HDACs. On the other hand, apicidin is a Class I HDAC inhibitor, inhibiting specifically HDAC1, 2 and 3 (46). To minimize secondary effects of HDAC inhibitors treatment, such as cell-cycle arrest or apoptosis, we limited treatment times

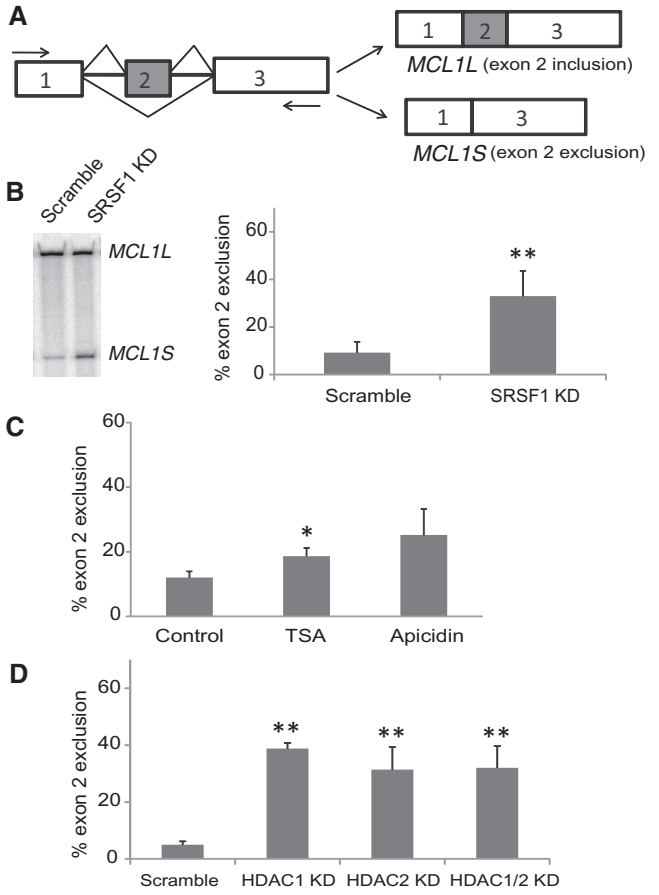

Figure 2. SRSF1, HDAC1 and HDAC2 regulate alternative splicing of *MCL1* RNA. (**A**) Schematic representation of *MCL1* alternative splicing. Arrows above and below map represent primers used in reverse transcription PCR (RT–PCR) assays. *MCL1* mature mRNAs were visualized and quantified on denaturing polyacrylamide gels after ^{32}P-labeling RT–PCR, in HCT116 cycling cells following (**B**) SRSF1 knockdown, (**C**) HDAC inhibitor (250 nM TSA or 150 nM apicidin) 2 h treatment or (**D**) HDAC1, HDAC2 or HDAC1/2 knockdown. Percentage of exon 2 exclusion was calculated by measuring the signal intensity of the spliced transcript (*MCL1S*) over the total transcripts (*MCL1S*+*MCL1L*). The average of at least three experiments is shown including SD, ** indicates $P \leq 0.01$ and *$P \leq 0.05$ of the *t*-test.

to a maximum of 2 h. In cycling HCT116 cells treated with TSA or apicidin for only 2 h, a shift in the splicing of the *MCL1* pre-mRNAs was observed in favor of *MCL1S* (Supplementary Figure S4B and Figure 2C). We repeated our studies with a natural HDAC inhibitor, butyrate at a physiologically relevant concentration (47,48) (Supplementary Figure S4C). With the use of three different HDAC inhibitors which are structurally unrelated and have different spectrum of substrate specificities, similar results were obtained (Figure 2C, Supplementary Figures S4B and S4C). Moreover, we tested the expression level of SRSF1 following treatment with HDAC inhibitors. Immunoblot analysis showed that the change in splicing resulting from HDAC inhibition was not due to a reduced expression of SRSF1. Up to 24 h treatment with TSA or apicidin did not affect SRSF1 protein levels (Supplementary Figure S4D). As SRSF1 is modified by acetylation (49), we probed its acetylation level with or without 2 h TSA or apicidin treatment. Reciprocal coimmunoprecipitation assays showed that the acetylation level of SRSF1 was not affected by HDAC inhibitors, while the histone H3 acetylation level was markedly increased (Supplementary Figure S4E). Thus, we were able to rule out an indirect effect of TSA or apicidin on *MCL1* splicing through differences in SRSF1 levels or SRSF1 acetylation. As a complementary approach and to specifically study the outcome of loss of HDAC1 and/or HDAC2 activity, we determined the effects of HDAC1, HDAC2 or HDAC1/HDAC2 knockdown on the *MCL1* splicing pattern. A representative immunoblot analysis of HDAC1 and/or HDAC2 knockdown in HCT116 cells is shown in Supplementary Figure S4F. HDAC1 knockdown was determined to be $78 \pm 1\%$ and $76 \pm 2\%$ in HDAC1 and HDAC1/2 knockdown HCT116 cells, respectively, while HDAC2 knockdown were $84 \pm 10\%$ and $85 \pm 12\%$ in HDAC2 and HDAC1/2 knockdown cells, respectively. We show that knockdown of either HDAC1 or HDAC2 or both led to a strongly significant change in splicing in favor of exon 2 skipping (Figures 2D and Supplementary Figure S4G). The immunoblot in Supplementary Figure S4F shows that the SRSF1 level was not affected by HDAC knockdown. These results indicate that HDAC1 and HDAC2 play a role in splice site selection by a mechanism other than altering expression or acetylation levels of SRSF1.

HDAC inhibitors affect the *MCL1* gene occupancy by RNAPII

The current literature supports the kinetic model where variation in RNAPII elongation rate or processivity modulates the splice site recognition efficiency. For genes with alternative exons that have weak splice sites, a slowly moving RNAPII results in the inclusion of the exons in the RNA (50). To investigate the effect of HDAC inhibitors (apicidin, TSA, butyrate) on the *MCL1* gene occupancy by the elongating form of RNAPII (RNAPIIS2ph), HDAC2, SRSF1 and acetylated histone, we performed dual crosslinking high resolution ChIP assays. Following a 2 h treatment of cycling HCT116 cells with the HDAC inhibitors, there was a reduced association with RNAPIIS2ph, HDAC2 and SRSF1 with the exon 2 nucleosome relative to nucleosomes at exon 1 and 3 (Supplementary Figures S5, S7 and S8). Also there was an increase in H3 and H4 acetylation of the exon 2 nucleosome (Supplementary Figures S6, S7 and S8). Meanwhile, results of H3 ChIP assays showing a uniform association of H3 along the *MCL1* gene with or without apicidin (Supplementary Figure S5) are consistent with ChIP assays being performed on mononucleosomes obtained by MNase digestion of chromatin (Supplementary Figure S5 and S7).

As dynamic acetylation results from the balance of opposing activities of HDACs and KATs, we turned our attention to KATs. A genome-wide mapping of several KATs revealed that p300 and CBP (KAT3A and B) as well as TAF1 (KAT4) were associated with promoter regions, while KAT2B (PCAF), KAT5 (TIP60) and

KAT8 (MOF) were located with transcribed regions (15). Moreover, KAT2B and KAT7 (HBO1) have been implicated in the elongation phase of transcription (51–53). Both KAT2B and KAT7 are H3 and H4 modifying enzymes (54). Hence, their distribution along the *MCL1* gene body was studied. The distributions of KAT2B and KAT7 were opposed to that of HDAC2, with an increased loading on exon 2 (Supplementary Figure S5 and S7).

Next we determined whether SRSF1 had a role in modulating the chromatin structure and/or the RNAPII elongation rate, which could lead to the change in splicing of *MCL1* transcripts. To this end, we compared the distributions of RNAPII, HDAC2 and acetylated histones along the *MCL1* gene in scramble and SRSF1 knockdown cells by ChIP assays. Under these conditions, no obvious changes in HDAC2 association, RNAPII distribution or acetylated histones were detected (Supplementary Figure S9). These results suggest that SRSF1 is involved in alternative splicing regulation of *MCL1* in a mechanism independent of the modulation of histone acetylation.

Effect of HDAC inhibitors on *MCL1* splicing is amplified upon TPA stimulation of serum-starved cells

Considering the observed consequences of HDAC inhibition on chromatin structure surrounding exon 2, the effects on splicing (Figure 2C) were rather small. This discrepancy was also observed previously and was interpreted as interference from the mRNA synthesized and spliced before HDAC inhibition (16). To alleviate this problem, the authors treated the cells with DRB, a reversible inhibitor of RNAPII, prior to HDAC inhibition. In this study, we exploited the transcriptional response of the *MCL1* gene downstream of the MAPK pathway (42) to study the effects of HDAC inhibitors on splicing during a synchronized induction of *MCL1* expression. Serum-starved HCT116 cells, pretreated or not for 30 min with apicidin or TSA, were stimulated with TPA. TPA stimulation of *MCL1* expression in control cells resulted in slight increase in exon 2 exclusion [see apicidin (−), TPA 60 min in Figure 3A; TSA (−), TPA 30 and 60 min in Supplementary Figure S10A]. With an increase in transcription initiation at the *MCL1* promoter, a higher density of elongating RNAPII was expected along the body of the gene. Indeed, RNAPIIS2ph ChIP assays revealed an increase in the number of RNAPII molecules along the body of the *MCL1* gene [see apicidin (−), TPA 60 min in Figure 3C; TSA (−), TPA 30 and 60 min in Supplementary Figure S10B]. This increased occupancy along the *MCL1* gene was also observed for SRSF1, HDAC2, KAT2B and KAT7 (Figure 3C and Supplementary Figure S10B), suggesting that all three proteins were associated with the elongating RNAPII complex. *MCL1* TPA stimulation was also accompanied by a global H3 and H4 acetylation (as well as H3K9ac, H3K14ac, H4K5ac and H4K8ac) increase along the body of the *MCL1* gene (Figures 4A, Supplementary Figures S11 and S12).

Besides interfering with dynamic acetylation of histones, HDAC inhibitors upregulate *MCL1* transcription (55). Thus, we analyzed the *MCL1* splicing pattern in serum-starved HCT116 cells submitted to a 30 min preincubation with apicidin or TSA, just prior to TPA induction. Similar to the TPA-induced control cells, apicidin- or TSA-treated cells had a slightly greater level of *MCL1* exon 2 exclusion than control cells [see apicidin (+), TPA 0 min in Figure 3A; TSA (+), TPA 0 min in Supplementary Figure S10A]. Apicidin- or TSA-treated cells also exhibited an increased occupancy of RNAPIIS2ph, SRSF1 and HDAC2 along the body of the *MCL1* gene compared to untreated cells, reflecting the HDAC inhibitor-induced upregulation of transcription initiation. However, at the same time, KAT2B and KAT7 started to associate specifically with exon 2. Moreover, a parallel exon 2-specific H3 and H4 acetylation increase was observed (Figures 4A, Supplementary Figures S11 and S12). So, after 30 min of inhibition of HDAC activity in serum-starved HCT116 cells, KAT2B and KAT7 have started to target the nucleosome positioned on the alternative exon.

Following TPA stimulation, apicidin and TSA had a profound impact on splicing, resulting in a marked increase of *MCL1* exon 2 exclusion [see apicidin (+), TPA 60 min in Figure 3A; TSA (+), TPA 30 and 60 min in Supplementary Figure S10A]. In the meantime, while RNAPIIS2ph on exon 1 increased as a consequence of TPA induction, the occupancy over exon 2 dropped dramatically, suggesting a sharp acceleration of the elongation process over exon 2. At exon 3, RNAPIIS2ph occupancy was similar to those on exon 1 [see apicidin (+), TPA 60 min in Figure 3C; TSA (+), TPA 30 and 60 min in Supplementary Figure S10B]. Moreover, the distribution of SRSF1 and HDAC2 on the body of the *MCL1* gene was consistent with these proteins being associated with RNAPIIS2ph. On the other hand, KAT2B and KAT7 levels rose sharply at exon 2 (Figures 3C and Supplementary Figure S10B), as did overall H3 and H4 acetylation, as well as H3K9ac, H3K14ac, H4K5ac, H4K8ac (Figures 4A, Supplementary Figures S11 and S12). It should be noted that changes at exon 2 were gradual changes occurring over time. This is particularly noticeable in the TSA-inhibition experiment (Supplementary Figures S10B and S12). As a control, the total H3 distribution along the body of the *MCL1* gene was analyzed. It was unaffected by TPA induction with or without apicidin or TSA treatment (Figures 3C and Supplementary Figure S10B).

Previous studies have demonstrated that H3 trimethylated at K4 was preferentially engaged in dynamic acetylation (15,56). In ChIP-sequencing studies, which determined the genomic distribution of H3K4me3 in HCT116 cells, we observed intense H3K4me3 at exon 2 of the *MCL1* gene (Figure 4B). This observation is in accordance with the selective histone acetylation of the exon 2 nucleosome, suggesting that the H3K4 methylated state of the exon 2 nucleosome has a role in recruiting KATs.

To recapitulate the above results, the TPA induction of *MCL1* expression was accompanied by an overall increase in density of RNAPIIS2ph and a slight increase in alternative exon 2 exclusion. On the other hand, the TPA induction of *MCL1* expression with HDAC inhibition led to gradual important local changes on exon 2 chromatin,

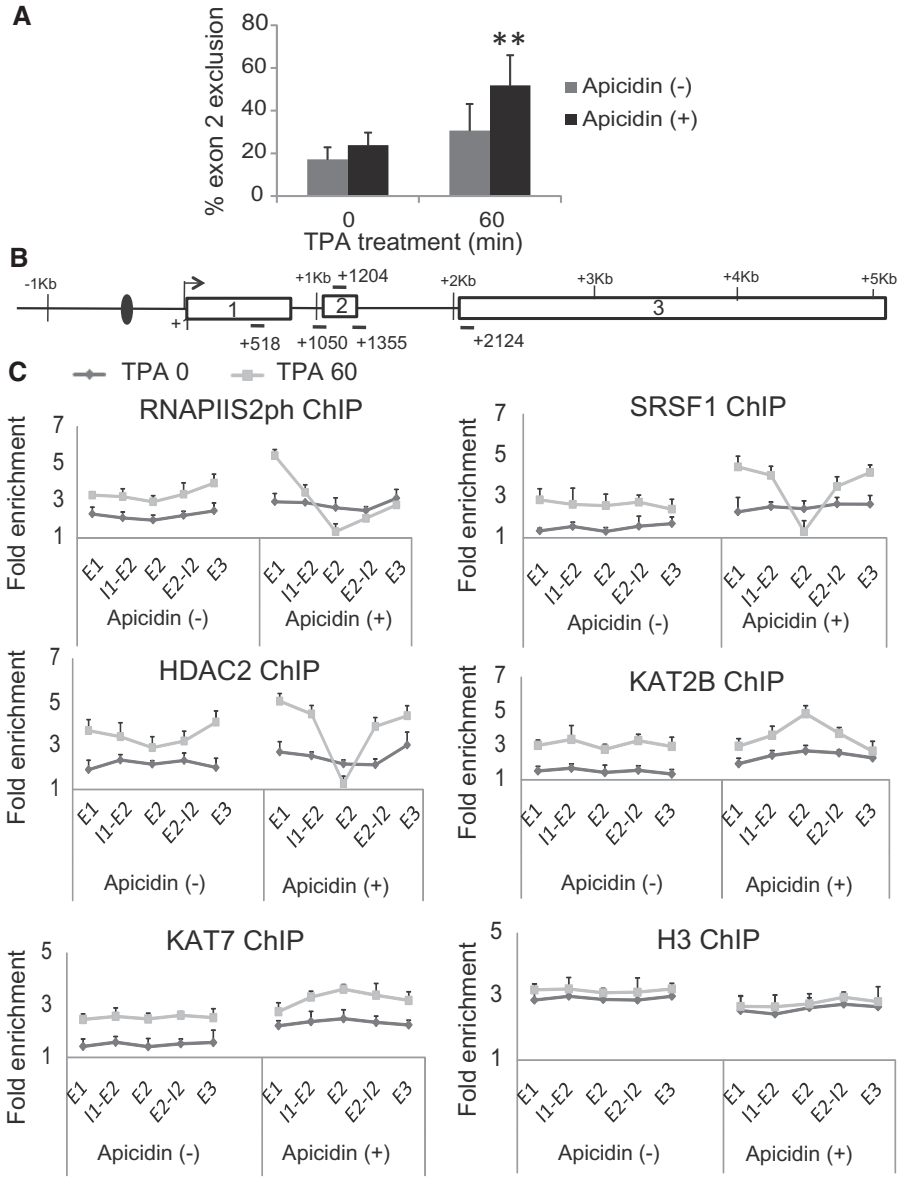

Figure 3. HDAC inhibition favors exclusion of alternative exon 2 upon TPA induction of *MCL1* gene. (**A**) *MCL1* alternative exon 2 splicing was analyzed in TPA-stimulated serum-starved HCT116 cells treated or not with 150 nM apicidin prior to TPA induction. (**B**) Schematic representation of the amplicons generated by real-time PCR analyses of ChIP DNA. (**C**) ChIP assays were performed on DSP- and formaldehyde-crosslinked mononucleosomes prepared from TPA-stimulated serum-starved HCT116 cells treated or not with 150 nM apicidin for 30 min prior to TPA induction.

resulting in exclusion of exon 2 from the pre-mRNA. Increased acetylation of H3 and H4 on nucleosome residing on exon 2 and targeting of KAT2B to exon 2 preceded the apicidin- or TSA-induced RNAPIIS2ph reduced occupancy over exon 2 [see apicidin (+), TPA 0 min in Figures 3C and 4A; TSA (+), TPA 0 min in Supplementary Figures S10B and S11]. These results suggest that the destabilization of the nucleosome over exon 2 leads to an increased elongation rate of this exon.

HDAC1, HDAC2 and KAT2B are associated with both the pre-mRNA and chromatin

ChIP assays have shown that the association of several splicing factors (SR proteins and HuR) to transcribed genes was sensitive to RNase treatment, indicating that these proteins bind more strongly to the pre-mRNA than to elongating RNAPII (17,41). To determine whether this was the case for SRSF1, we performed ChIP assays on DSP- and formaldehyde-crosslinked mononucleosomes prepared from lysates of TPA-stimulated serum-starved HCT116 cells, which were treated or not with RNase A prior to the immunoprecipitation step. Our results show that RNase treatment of dual crosslinked mononucleosomes reduced the association of SRSF1 with the body of the *MCL1* gene in serum-starved and TPA-stimulated HCT116 cells (Figure 5A), suggesting that SRSF1 was bound to the pre-mRNA. As HDAC2 is corecruited with SRSF1 to the body of transcribed genes, we repeated our ChIP

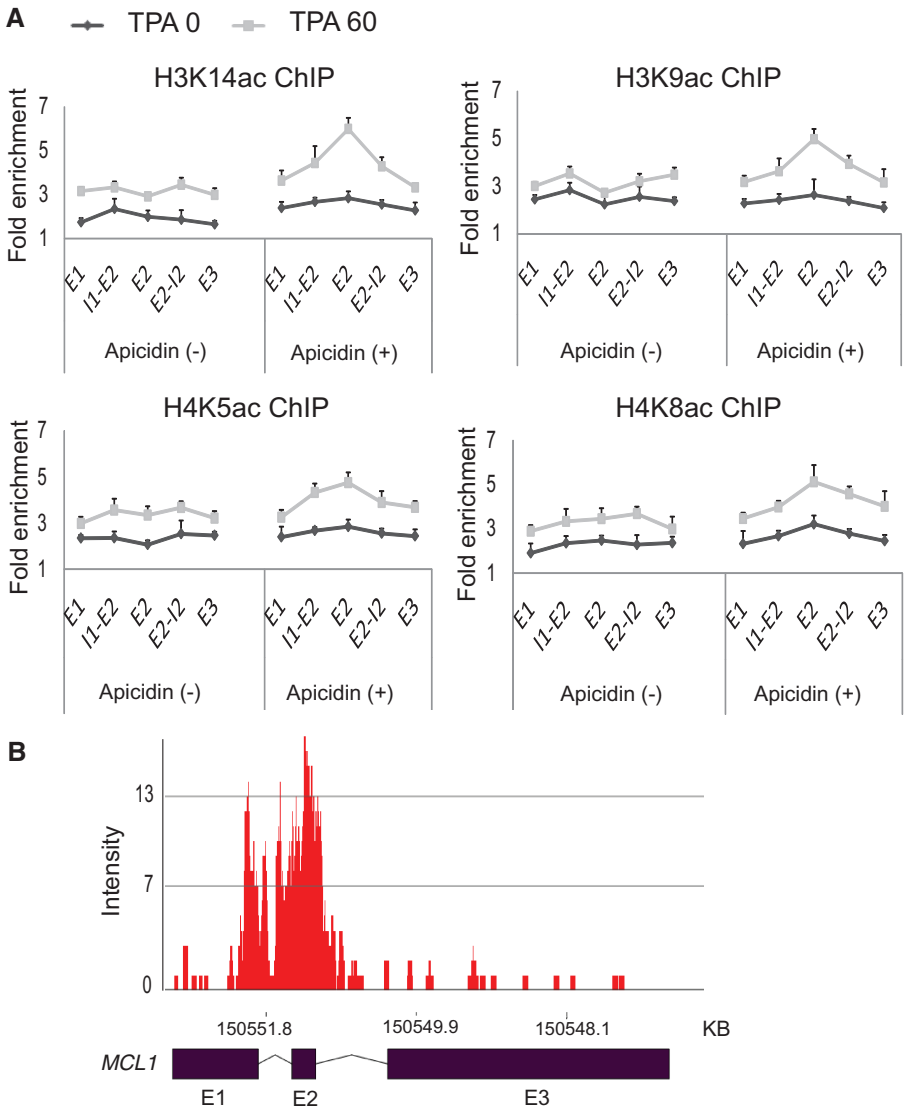

Figure 4. Specific enrichment of H3 and H4 acetylation and methylation over *MCL1* exon 2. (**A**) HDAC inhibition specifically increases H3 and H4 acetylation over exon 2 upon TPA induction of *MCL1* gene. ChIP experiments were performed as described in Figure 3. (**B**) ChIP-sequencing determined H3K4me3 signals along the *MCL1* gene were displayed by Partek Genomic Suite. The Y-axis is the signal intensity of mapped sequence reads.

assay with antibodies against HDAC2. Figure 5A shows that HDAC2 association with *MCL1* was markedly reduced upon RNase digestion, suggesting that HDAC2 interacted with the *MCL1* pre-mRNA.

It was shown that SRSF1 interaction with RNAPIIS2ph was also mediated by the pre-mRNA given that it was sensitive to RNase as opposed to a direct protein–protein interaction, which would be RNase-insensitive. We set out to confirm this finding in HCT116 cells and find out if HDAC2 also formed a RNase-sensitive cotranscriptional complex with RNAPIIS2ph. Thus, we carried out reciprocal coimmunoprecipitation assays using HCT116 cell lysates treated or not with RNase A. Figure 5B shows that SRSF1 interaction with RNAPIIS2ph was RNA-dependent as SRSF1 did not coimmunoprecipitate with RNAPIIS2ph in the presence of RNase A, and vice versa (Supplementary Figure S13). Similar results were obtained for HDAC2 and RNAPIIS2ph interactions (Figures 5B and Supplementary Figure S13).

To confirm the association of SRSF1 and HDAC2 with the *MCL1* mRNA, we used the CLIP (ultraviolet crosslinking and immunoprecipitation) method to analyze their *in situ* direct binding to RNA. We also investigated the interactions of HDAC1 and KAT2B with RNA, as KAT2B had been reported to associate with RNAPII, in complex with hnRNP U and actin (52). RNP complexes in cycling HCT116 cells, treated or not for 2 h with apicidin or TSA, were covalently crosslinked by UV exposure only or by DSP and UV exposure, and RNA complexes were immunopurified with anti-SRSF1, anti-HDAC1, anti-HDAC2 or anti-KAT2B antibodies. In UV-treated cells, RT-PCR analysis showed a significant enrichment of *MCL1* exon 1, exon 2 and exon 3 mRNAs in SRSF1 immunoprecipitation versus an irrelevant IgG control, but the

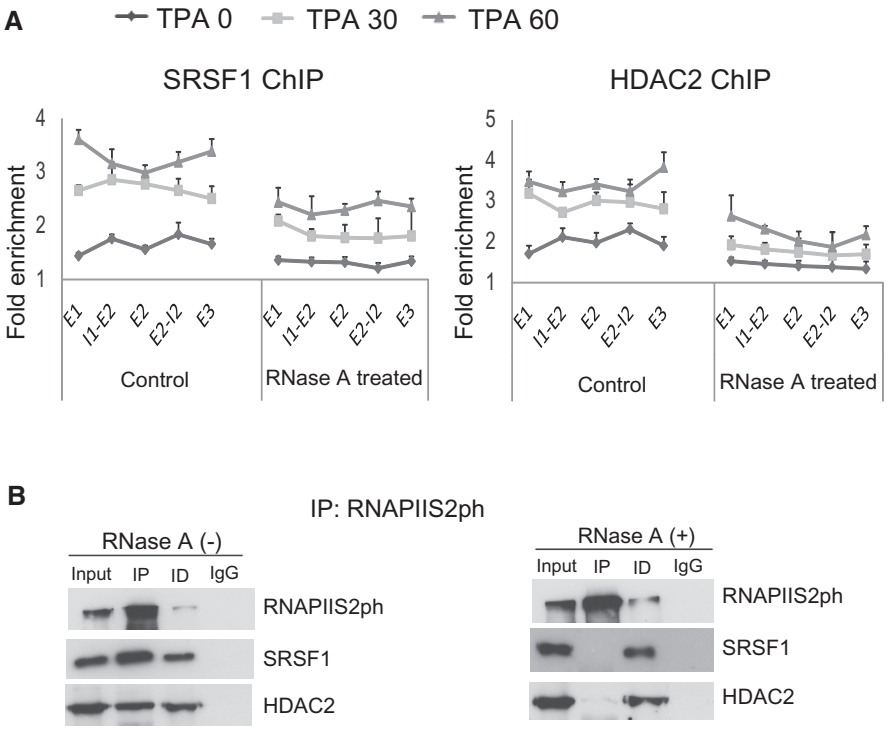

Figure 5. SRSF1 and HDAC2 recruitment to *MCL1* gene body and their interactions with RNAPII are RNA-dependent. (**A**) ChIP experiments were performed on DSP- and formaldehyde-crosslinked mononucleosomes prepared from lysates of serum-starved HCT116 cells stimulated with 100 nM TPA for 0, 30 or 60 min. Lysates were treated or not with RNase A. (**B**) SRSF1 and HDAC2 interactions with RNAPIIS2ph are dependent on RNA. HCT116 cell lysates treated or not with RNase A were incubated with anti-RNAPIIS2ph antibody. Immunoprecipitated (IP) and immunodepleted (ID) fractions were analyzed by immunoblot assay for the presence of indicated proteins. Isotype specific nonrelated IgGs were used as negative control.

enrichments in HDAC1, HDAC2 or KAT2B immunoprecipitations were minimal for all three exon mRNAs (Figure 6). On the other hand, when RNP complexes were crosslinked by DSP and UV exposure, there was a significant enrichment of *MCL1* exon 1, exon 2 and exon 3 mRNAs in each of the immunoprecipitations versus an IgG control. The results were independent of HDAC activity, as they were not affected by the treatment of cells with HDAC inhibitors apicidin or TSA (Figure 6). The detection of significant HDAC1, HDAC2 and KAT2B association with the *MCL1* mRNA being dependent on dual crosslinking indicates that the interactions of these proteins with the mRNA are indirect and are mediated by splicing factors.

Together, these results are consistent with the idea that HDAC1, HDAC2 and KAT2B are associated with the pre-mRNA while catalyzing the dynamic acetylation of *MCL1* chromatin.

DISCUSSION

Nucleosomes are nonuniformly distributed along the body of transcribed genes and are enriched on exons relative to introns. Notably, the average length of human internal exons is very close to the length of DNA within a nucleosome (147 bp). This marked correspondence also applies to six other tested metazoans (57,58), suggesting a conserved role for the nucleosome in exon definition and

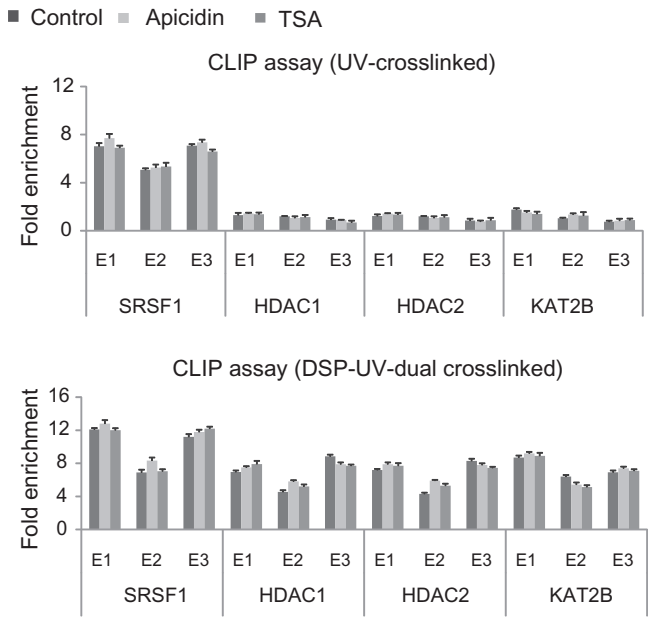

Figure 6. SRSF1, HDAC1, HDAC2 and KAT2B recruitment to *MCL1* gene body is mediated by pre-mRNA. Immunoprecipitations with indicated antibodies were performed on UV light-exposed or dual DSP and UV light crosslinked RNP complexes isolated from HCT116 cycling cells. Reverse transcription PCR measurements were normalized to the value obtained with IgG control antibodies.

splicing regulation. Our studies demonstrate that the nucleosome positioned over the alternative exon 2 of the *MCL1* gene is highly dynamic with regard to histone acetylation, a state which greatly impacts on splicing decision.

Our mass spectrometry data showed that HDAC1 and HDAC2, more accurately nonphosphorylated HDAC2, coimmunoprecipitated with numerous splicing factors. Interestingly mass spectrometry analyses of the spliceosome had identified HDAC2 as a component of this complex (59). SR proteins associate with chromatin in a transcription-dependent manner (41), and we show that HDAC1 and HDAC2 are co-chromatin immunoprecipitated with SRSF1 along the body of genes upon transcription induction, regardless of whether the transcripts of these genes are constitutively or alternatively spliced. The presence of SRSF1 in the HDAC1 and HDAC2 immunoprecipitate did not inhibit HDAC activity as the SRSF1/HDAC1 and SRSF1/HDAC2 immunoprecipitates had deacetylase activity. Of note, we repeated the *in vitro* experiment showing that HuR proteins inhibit the HDAC activity in a HDAC2 immunoprecipitate from HeLa nuclear extracts (17), but contrary to what was published, we found no impact of the HuR protein on HDAC activity. It was proposed that SRSF1 is recruited to transcribed genes by RNAPII upon stimulation of elongation, which occurs with the LARP7 (P-TEFb)-mediated phosphorylation of the CTD of RNAPII at Ser 2 (40). It is most likely that HDAC1 and HDAC2 are recruited at the same time, in association with splicing factors. This model is supported by our data showing that HDAC2 interactions with numerous splicing factors are unaffected by RNase treatment. Furthermore, SRSF1 knockdown did not affect the recruitment of HDAC1 and HDAC2 to the body of the *MCL1* gene or the *TFF1* gene upon its induction (data not shown). Also the increased *MCL1* exon 2 exclusion resulting from a SRSF1 knockdown did not affect *MCL1* exon 2 acetylation or the RNAPII distribution along the *MCL1* gene (60), suggesting that SRSF1 affects *MCL1* splicing through a mechanism which is not dependent on modulation of histone acetylation. Since HDAC1 and HDAC2 are associated with so many splicing proteins, it is not surprising that their recruitment to the body of a transcribed gene is not affected by the knockdown of one of them. Vice-versa, HDAC1 and/or HDAC2 knockdown did not affect SRSF1 recruitment to the *TFF1* gene.

SR proteins interact with the nascent pre-mRNA, RNAPIIS2ph and chromatin. SR proteins interactions with RNAPIIS2ph are RNase-sensitive, indicating that they are RNA mediated. On the other hand, SR proteins interactions with chromatin were reduced by RNase treatment, but not abolished, suggesting that these interactions are partially mediated by RNA (41). Indeed, in the case of SRSF1, interaction with chromatin also occurs via the tail of nucleosomal histone H3 (61). In this study, we show for the first time that HDAC1 and HDAC2 also reside on the pre-mRNA. In fact, the association of HDAC2 with the body of the *MCL1* gene was particularly sensitive to RNase, more so than the association of SRSF1. Likewise, HDAC2 association with RNAPIIS2ph was RNA-dependent, indicating that HDAC2 was not bound directly to RNAPIIS2ph. Our results demonstrating that HDAC1 and HDAC2 are associated with the emerging RNA transcripts are supported by our previous ChIP experiments, in which we needed to use dual crosslinking to monitor HDAC1 and HDAC2 along the body of genes; formaldehyde alone worked poorly (12). Likewise, a genome wide-mapping study of KATs and HDACs applied dual crosslinking (15). In agreement with previous results revealing that KAT2B is associated with RNAPII, in complex with hnRNP U and actin (52), we show that KAT2B is bound to the pre-mRNA. We propose that HDAC1 and HDAC2, in concert with KAT2B, and other KATs, catalyze nucleosomal dynamic acetylation by acting at the RNA level.

Evidence is accumulating to show the importance of nuclear RNA in maintaining the structure of transcribed chromatin as well as the nuclear location of transcribed genes (62–65). It is quite possible that nuclear RNA associated with regulatory and coding regions of transcribed and silent chromatin domains serves as a platform for several chromatin-modifying enzymes.

It is interesting to note that the ENCODE ChIP-sequencing data show that H3K4me3 peaks at the *MCL1* exon 2 in many cell types (66,67). There are several mechanisms by which the exon 2 nucleosome H3K4me3 mark recruits KAT2B and KAT7. KAT2B is a component of the SAGA and ATAC complexes which contain the SAGA-associated factor 29, which binds to H3K4me3 (68,69). Similarly the ING4 subunit of the KAT7 complex binds to H3K4me3 (70). The histone acetylation activity of the KATs is countered by the HDACs. It should be noted that in cycling cells, the steady state levels of H3K9ac and H3K14ac at exon 2 are decreased compared with the rest of the *MCL1* gene body. This observation suggests that HDAC activity is locally increased relative to KAT activity on exon 2.

Our data show that the recruitment of KATs to exon 2 and increased acetylation of exon 2 nucleosome precedes locally decreased RNAPII occupancy, implying that increased nucleosomal acetylation contributes to faster elongation. This conclusion is supported by an *in vitro* transcriptional elongation experiments showing that acetylation of H3 and H4 tails overcomes the inhibitory effect of nucleosomes (71). *In situ* experiments have also demonstrated that histone acetylation is required to maintain the unfolded structure of the transcribed nucleosome (72). It is assumed that histone acetylation facilitates subsequent rounds of transcription elongation (73).

Upon HDAC inhibition or knockdown (HDAC1 and/or 2), exon 2 nucleosome acetylation markedly increases due to the H3K4me3 localized KAT activity. Within 30 min of HDAC inhibition, an enhanced recruitment of KAT2B and KAT7 to *MCL1* exon 2 was observed. Recruitment of the KAT may escalate through their binding to acetylated H3 and H4 through the enzyme's bromodomain (74). By binding to the product of its activity, KAT2B occupancy could be self-reinforcing.

SR proteins regulate alternative splicing by binding to exonic splicing enhancers and enhancing U1 snRNP and

U2 snRNP recruitment, thus promoting recognition of exons with suboptimal splice sites (41). In agreement with this mode of action, we and others (45) found that SRSF1 knockdown resulted in increased *MCL1* exon 2 exclusion. Enzymatic inhibition of HDACs (three HDAC inhibitors, TSA, apicidin and butyrate that are structurally unrelated and have different substrate spectra) or siRNA-mediated knockdown of HDAC1 and/or HDAC2 also resulted in increased *MCL1* exon 2 exclusion, without affecting SRSF1 levels. Of these HDAC inhibitors, butyrate produced by fermentation of dietary fiber by colonic bacteria could reach sufficient levels (0.5–5 mM) to alter *MCL1* splicing in colonic cells (47,48). Following HDAC inhibition, the hyperacetylation of *MCL1* exon 2 nucleosome and increased elongation rate may result in an altered localization and decreased recruitment of SRSF1 and other splicing factors to the *MCL1* transcript (23). These events could explain the loss of association of SRSF1 and HDAC1/2 with the hyperacetylated *MCL1* exon 2 nucleosome in our ChIP assays (23). Thus, although acting through different mechanisms, HDAC inhibitors and SRSF1 knockdown prevent the SRSF1-mediated exon 2 inclusion (23).

Future studies will determine the role of H3K4 methylation and dynamic histone acetylation in regulating alternative RNA splicing. We propose that HDAC inhibitors will alter pre-mRNA splicing when nucleosomes placed at regions containing alternative exons are modified by H3K4 methylation. The nucleosomes marked by H3K4 methylation are preferentially engaged in dynamic acetylation (15,56). Hence HDAC inhibition may increase elongation rates at the alternative exon and alter the association of splicing factors to the transcript, resulting in exon exclusion or inclusion (23). To conclude, our results highlight the roles of HDACs and KATs in regulating the interface between chromatin organization and alternative splicing.

SUPPLEMENTARY DATA

Supplementary Data are available at NAR Online.

ACKNOWLEDGEMENTS

The authors thank Nehal Patel and Wenguang Cao for technical assistance and Geneviève Delcuve for writing the manuscript.

FUNDING

The Canadian Institutes of Health Research [MOP-9186 J.R.D.]; Canadian Breast Cancer Foundation (to J.R.D. and E.L.); Manitoba Health Research Council (to E.L.); CancerCare Manitoba Foundation (to E.L.); National Institutes of Health [1R01 GM047867 to J.L.W.]; Stowers Institute for Medical Research (to J.L.W.); Canada Research Chair (to J.R.D.); MHRC/CancerCare Manitoba studentship (to D.H.K.); MHRC postdoctoral fellowship (to S.H.); Manitoba Institute of Child Health and CancerCare Manitoba Foundation; Manitoba Next Generation Sequencing Platform was supported by generous funds from the Canadian Foundation for Innovation, Province of Manitoba, University of Manitoba Faculty of Medicine, Manitoba Health Research Council, CancerCare Manitoba Foundation, Manitoba Institute of Child Health, and Manitoba Institute of Cell Biology. Funding for open access charge: Canadian Institutes of Health Research and Canadian Breast Cancer Foundation.

REFERENCES

1. Barlev,N.A., Liu,L., Chehab,N.H., Mansfield,K., Harris,K.G., Halazonetis,T.D. and Berger,S.L. (2001) Acetylation of p53 activates transcription through recruitment of coactivators/histone acetyltransferases. *Mol. Cell*, **8**, 1243–1254.
2. Hubbert,C., Guardiola,A., Shao,R., Kawaguchi,Y., Ito,A., Nixon,A., Yoshida,M., Wang,X.F. and Yao,T.P. (2002) HDAC6 is a microtubule-associated deacetylase. *Nature*, **417**, 455–458.
3. Katan-Khaykovich,Y. and Struhl,K. (2002) Dynamics of global histone acetylation and deacetylation in vivo: rapid restoration of normal histone acetylation status upon removal of activators and repressors. *Genes Dev.*, **16**, 743–752.
4. Martinez-Balbas,M.A., Bauer,U.M., Nielsen,S.J., Brehm,A. and Kouzarides,T. (2000) Regulation of E2F1 activity by acetylation. *EMBO J.*, **19**, 662–671.
5. Yao,Y.L., Yang,W.M. and Seto,E. (2001) Regulation of transcription factor YY1 by acetylation and deacetylation. *Mol. Cell Biol.*, **21**, 5979–5991.
6. Zhang,D.-E. and Nelson,D.A. (1988) Histone acetylation in chicken erythrocytes: rates of deacetylation in immature and mature red blood cells. *Biochem. J.*, **250**, 241–245.
7. Zhang,D.-E. and Nelson,D.A. (1988) Histone acetylation in chicken erythrocytes: rates of acetylation and evidence that histones in both active and potentially active chromatin are rapidly modified. *Biochem. J.*, **250**, 233–240.
8. Li,Y., Kimura,T., Huyck,R.W., Laity,J.H. and Andrews,G.K. (2008) Zinc-induced formation of a coactivator complex containing the zinc-sensing transcription factor MTF-1, p300/CBP, and Sp1. *Mol. Cell Biol.*, **28**, 4275–4284.
9. Masumi,A., Wang,I.M., Lefebvre,B., Yang,X.J., Nakatani,Y. and Ozato,K. (1999) The histone acetylase PCAF is a phorbol-ester-inducible coactivator of the IRF family that confers enhanced interferon responsiveness. *Mol. Cell Biol.*, **19**, 1810–1820.
10. Taubert,S., Gorrini,C., Frank,S.R., Parisi,T., Fuchs,M., Chan,H.M., Livingston,D.M. and Amati,B. (2004) E2F-dependent histone acetylation and recruitment of the Tip60 acetyltransferase complex to chromatin in late G1. *Mol. Cell Biol.*, **24**, 4546–4556.
11. Sun,J.M., Chen,H.Y., Moniwa,M., Litchfield,D.W., Seto,E. and Davie,J.R. (2002) The transcriptional repressor Sp3 is associated with CK2 phosphorylated histone deacetylase 2. *J. Biol. Chem.*, **277**, 35783–35786.
12. Sun,J.M., Chen,H.Y. and Davie,J.R. (2007) Differential distribution of unmodified and phosphorylated histone deacetylase 2 in chromatin. *J. Biol. Chem.*, **282**, 33227–33236.
13. Tsai,S.C. and Seto,E. (2002) Regulation of histone deacetylase 2 by protein kinase CK2. *J. Biol. Chem.*, **277**, 31826–31833.
14. Pflum,M.K., Tong,J.K., Lane,W.S. and Schreiber,S.L. (2001) Histone deacetylase 1 phosphorylation promotes enzymatic activity and complex formation. *J. Biol. Chem.*, **276**, 47733–47741.
15. Wang,Z., Zang,C., Cui,K., Schones,D.E., Barski,A., Peng,W. and Zhao,K. (2009) Genome-wide mapping of HATs and HDACs reveals distinct functions in active and inactive genes. *Cell*, **138**, 1019–1031.
16. Hnilicova,J., Hozeifi,S., Duskova,E., Icha,J., Tomankova,T. and Stanek,D. (2011) Histone deacetylase activity modulates alternative splicing. *PLoS One*, **6**, e16727.
17. Zhou,H.L., Hinman,M.N., Barron,V.A., Geng,C., Zhou,G., Luo,G., Siegel,R.E. and Lou,H. (2011) Hu proteins regulate alternative splicing by inducing localized histone hyperacetylation

in an RNA-dependent manner. *Proc. Natl Acad. Sci. USA*, **108**, E627–E635.
18. Castle,J.C., Zhang,C., Shah,J.K., Kulkarni,A.V., Kalsotra,A., Cooper,T.A. and Johnson,J.M. (2008) Expression of 24,426 human alternative splicing events and predicted cis regulation in 48 tissues and cell lines. *Nat. Genet.*, **40**, 1416–1425.
19. Kalsotra,A., Xiao,X., Ward,A.J., Castle,J.C., Johnson,J.M., Burge,C.B. and Cooper,T.A. (2008) A postnatal switch of CELF and MBNL proteins reprograms alternative splicing in the developing heart. *Proc. Natl Acad. Sci. USA*, **105**, 20333–20338.
20. Wang,E.T., Sandberg,R., Luo,S., Khrebtukova,I., Zhang,L., Mayr,C., Kingsmore,S.F., Schroth,G.P. and Burge,C.B. (2008) Alternative isoform regulation in human tissue transcriptomes. *Nature*, **456**, 470–476.
21. de la Mata,M., Alonso,C.R., Kadener,S., Fededa,J.P., Blaustein,M., Pelisch,F., Cramer,P., Bentley,D. and Kornblihtt,A.R. (2003) A slow RNA polymerase II affects alternative splicing in vivo. *Mol. Cell*, **12**, 525–532.
22. Ip,J.Y., Schmidt,D., Pan,Q., Ramani,A.K., Fraser,A.G., Odom,D.T. and Blencowe,B.J. (2011) Global impact of RNA polymerase II elongation inhibition on alternative splicing regulation. *Genome Res.*, **21**, 390–401.
23. Schor,I.E., Lleres,D., Risso,G.J., Pawellek,A., Ule,J., Lamond,A.I. and Kornblihtt,A.R. (2012) Perturbation of chromatin structure globally affects localization and recruitment of splicing factors. *PLoS One*, **7**, e48084.
24. Luco,R.F., Pan,Q., Tominaga,K., Blencowe,B.J., Pereira-Smith,O.M. and Misteli,T. (2010) Regulation of alternative splicing by histone modifications. *Science*, **327**, 996–1000.
25. Zhou,H.L., Luo,G., Wise,J.A. and Lou,H. (2014) Regulation of alternative splicing by local histone modifications: potential roles for RNA-guided mechanisms. *Nucleic Acids Res.*, **42**, 701–713.
26. Adami,G. and Babiss,L.E. (1991) DNA template effect on RNA splicing: two copies of the same gene in the same nucleus are processed differently. *EMBO J.*, **10**, 3457–3465.
27. Kim,S., Kim,H., Fong,N., Erickson,B. and Bentley,D.L. (2011) Pre-mRNA splicing is a determinant of histone H3K36 methylation. *Proc. Natl Acad. Sci. USA*, **108**, 13564–13569.
28. Saint-Andre,V., Batsche,E., Rachez,C. and Muchardt,C. (2011) Histone H3 lysine 9 trimethylation and HP1gamma favor inclusion of alternative exons. *Nat. Struct. Mol. Biol.*, **18**, 337–344.
29. Schor,I.E., Rascovan,N., Pelisch,F., Allo,M. and Kornblihtt,A.R. (2009) Neuronal cell depolarization induces intragenic chromatin modifications affecting NCAM alternative splicing. *Proc. Natl Acad. Sci. USA*, **106**, 4325–4330.
30. Sims,R.J. III, Millhouse,S., Chen,C.F., Lewis,B.A., Erdjument-Bromage,H., Tempst,P., Manley,J.L. and Reinberg,D. (2007) Recognition of trimethylated histone H3 lysine 4 facilitates the recruitment of transcription postinitiation factors and pre-mRNA splicing. *Mol. Cell*, **28**, 665–676.
31. Kadener,S., Cramer,P., Nogues,G., Cazalla,D., de la,M.M., Fededa,J.P., Werbajh,S.E., Srebrow,A. and Kornblihtt,A.R. (2001) Antagonistic effects of T-Ag and VP16 reveal a role for RNA pol II elongation on alternative splicing. *EMBO J.*, **20**, 5759–5768.
32. Sanford,J.R., Wang,X., Mort,M., Vanduyn,N., Cooper,D.N., Mooney,S.D., Edenberg,H.J. and Liu,Y. (2009) Splicing factor SFRS1 recognizes a functionally diverse landscape of RNA transcripts. *Genome Res.*, **19**, 381–394.
33. Bae,J., Leo,C.P., Hsu,S.Y. and Hsueh,A.J. (2000) MCL-1S, a splicing variant of the antiapoptotic BCL-2 family member MCL-1, encodes a proapoptotic protein possessing only the BH3 domain. *J. Biol. Chem.*, **275**, 25255–25261.
34. Meng,X. and Wilkins,J.A. (2005) Compositional characterization of the cytoskeleton of NK-like cells. *J. Proteome. Res.*, **4**, 2081–2087.
35. Drobic,B., Perez-Cadahia,B., Yu,J., Kung,S.K. and Davie,J.R. (2010) Promoter chromatin remodeling of immediate-early genes is mediated through H3 phosphorylation at either serine 28 or 10 by the MSK1 multi-protein complex. *Nucleic Acids Res.*, **38**, 3196–3208.
36. Zhang,Y., Liu,T., Meyer,C.A., Eeckhoute,J., Johnson,D.S., Bernstein,B.E., Nusbaum,C., Myers,R.M., Brown,M., Li,W. *et al.* (2008) Model-based analysis of ChIP-Seq (MACS). *Genome Biol.*, **9**, R137.
37. Shin,H., Liu,T., Manrai,A.K. and Liu,X.S. (2009) CEAS: cis-regulatory element annotation system. *Bioinformatics*, **25**, 2605–2606.
38. Khan,D.H., He,S., Yu,J., Winter,S., Cao,W., Seiser,C. and Davie,J.R. (2013) Protein kinase CK2 regulates the dimerization of histone deacetylase (HDAC) 1 and HDAC2 during mitosis. *J. Biol. Chem.*, **288**, 16518–16528.
39. Cho,S., Hoang,A., Chakrabarti,S., Huynh,N., Huang,D.B. and Ghosh,G. (2011) The SRSF1 linker induces semi-conservative ESE binding by cooperating with the RRMs. *Nucleic Acids Res.*, **39**, 9413–9421.
40. Barboric,M., Lenasi,T., Chen,H., Johansen,E.B., Guo,S. and Peterlin,B.M. (2009) 7SK snRNP/P-TEFb couples transcription elongation with alternative splicing and is essential for vertebrate development. *Proc. Natl Acad. Sci. USA*, **106**, 7798–7803.
41. Sapra,A.K., Anko,M.L., Grishina,I., Lorenz,M., Pabis,M., Poser,I., Rollins,J., Weiland,E.M. and Neugebauer,K.M. (2009) SR protein family members display diverse activities in the formation of nascent and mature mRNPs in vivo. *Mol. Cell*, **34**, 179–190.
42. Booy,E.P., Henson,E.S. and Gibson,S.B. (2011) Epidermal growth factor regulates Mcl-1 expression through the MAPK-Elk-1 signalling pathway contributing to cell survival in breast cancer. *Oncogene*, **30**, 2367–2378.
43. Pentecost,B.T., Bradley,L.M., Gierthy,J.F., Ding,Y. and Fasco,M.J. (2005) Gene regulation in an MCF-7 cell line that naturally expresses an estrogen receptor unable to directly bind DNA. *Mol. Cell Endocrinol.*, **238**, 9–25.
44. Espino,P.S., Li,L., He,S., Yu,J. and Davie,J.R. (2006) Chromatin modification of the trefoil factor 1 gene in human breast cancer cells by the Ras/mitogen-activated protein kinase pathway. *Cancer Res.*, **66**, 4610–4616.
45. Moore,M.J., Wang,Q., Kennedy,C.J. and Silver,P.A. (2010) An alternative splicing network links cell-cycle control to apoptosis. *Cell*, **142**, 625–636.
46. Bantscheff,M., Hopf,C., Savitski,M.M., Dittmann,A., Grandi,P., Michon,A.M., Schlegl,J., Abraham,Y., Becher,I., Bergamini,G. *et al.* (2011) Chemoproteomics profiling of HDAC inhibitors reveals selective targeting of HDAC complexes. *Nat. Biotechnol.*, **29**, 255–265.
47. Donohoe,D.R., Collins,L.B., Wali,A., Bigler,R., Sun,W. and Bultman,S.J. (2012) The Warburg effect dictates the mechanism of butyrate-mediated histone acetylation and cell proliferation. *Mol. Cell*, **48**, 612–626.
48. Donohoe,D.R., Curry,K.P. and Bultman,S.J. (2013) Microbial oncotarget: bacterial-produced butyrate, chemoprevention and Warburg effect. *Oncotarget.*, **4**, 182–183.
49. Choudhary,C., Kumar,C., Gnad,F., Nielsen,M.L., Rehman,M., Walther,T.C., Olsen,J.V. and Mann,M. (2009) Lysine acetylation targets protein complexes and co-regulates major cellular functions. *Science*, **325**, 834–840.
50. Carrillo Oesterreich,F., Bieberstein,N. and Neugebauer,K.M. (2011) Pause locally, splice globally. *Trends Cell Biol.*, **21**, 328–335.
51. Cho,H., Orphanides,G., Sun,X., Yang,X.J., Ogryzko,V., Lees,E., Nakatani,Y. and Reinberg,D. (1998) A human RNA polymerase II complex containing factors that modify chromatin structure. *Mol. Cell Biol.*, **18**, 5355–5363.
52. Obrdlik,A., Kukalev,A., Louvet,E., Farrants,A.K., Caputo,L. and Percipalle,P. (2008) The histone acetyltransferase PCAF associates with actin and hnRNP U for RNA polymerase II transcription. *Mol. Cell Biol.*, **28**, 6342–6357.
53. Saksouk,N., Avvakumov,N., Champagne,K.S., Hung,T., Doyon,Y., Cayrou,C., Paquet,E., Ullah,M., Landry,A.J., Cote,V. *et al.* (2009) HBO1 HAT complexes target chromatin throughout gene coding regions via multiple PHD finger interactions with histone H3 tail. *Mol. Cell*, **33**, 257–265.
54. Lee,K.K. and Workman,J.L. (2007) Histone acetyltransferase complexes: one size doesn't fit all. *Nat. Rev. Mol. Cell Biol.*, **8**, 284–295.

55. Inoue,S., Walewska,R., Dyer,M.J. and Cohen,G.M. (2008) Downregulation of Mcl-1 potentiates HDACi-mediated apoptosis in leukemic cells. *Leukemia*, **22**, 819–825.
56. Hazzalin,C.A. and Mahadevan,L.C. (2005) Dynamic acetylation of all lysine 4-methylated histone H3 in the mouse nucleus: analysis at c-fos and c-jun. *PLoS. Biol.*, **3**, e393.
57. Schwartz,S., Meshorer,E. and Ast,G. (2009) Chromatin organization marks exon-intron structure. *Nat. Struct. Mol. Biol.*, **16**, 990–995.
58. Tilgner,H., Nikolaou,C., Althammer,S., Sammeth,M., Beato,M., Valcarcel,J. and Guigo,R. (2009) Nucleosome positioning as a determinant of exon recognition. *Nat. Struct. Mol. Biol.*, **16**, 996–1001.
59. Rappsilber,J., Ryder,U., Lamond,A.I. and Mann,M. (2002) Large-scale proteomic analysis of the human spliceosome. *Genome Res.*, **12**, 1231–1245.
60. Ji,X., Zhou,Y., Pandit,S., Huang,J., Li,H., Lin,C.Y., Xiao,R., Burge,C.B. and Fu,X.D. (2013) SR proteins collaborate with 7SK and promoter-associated nascent RNA to release paused polymerase. *Cell*, **153**, 855–868.
61. Loomis,R.J., Naoe,Y., Parker,J.B., Savic,V., Bozovsky,M.R., Macfarlan,T., Manley,J.L. and Chakravarti,D. (2009) Chromatin binding of SRp20 and ASF/SF2 and dissociation from mitotic chromosomes is modulated by histone H3 serine 10 phosphorylation. *Mol. Cell*, **33**, 450–461.
62. Caudron-Herger,M., Muller-Ott,K., Mallm,J.P., Marth,C., Schmidt,U., Fejes-Toth,K. and Rippe,K. (2011) Coding RNAs with a non-coding function: maintenance of open chromatin structure. *Nucleus*, **2**, 410–424.
63. Khalil,A.M., Guttman,M., Huarte,M., Garber,M., Raj,A., Rivea,M.D., Thomas,K., Presser,A., Bernstein,B.E., van,O.A. *et al.* (2009) Many human large intergenic noncoding RNAs associate with chromatin-modifying complexes and affect gene expression. *Proc. Natl Acad. Sci. USA*, **106**, 11667–11672.
64. Mitchell,J.A., Clay,I., Umlauf,D., Chen,C.Y., Moir,C.A., Eskiw,C.H., Schoenfelder,S., Chakalova,L., Nagano,T. and Fraser,P. (2012) Nuclear RNA sequencing of the mouse erythroid cell transcriptome. *PLoS One*, **7**, e49274.
65. Rodriguez-Campos,A. and Azorin,F. (2007) RNA is an integral component of chromatin that contributes to its structural organization. *PLoS One*, **2**, e1182.
66. Rosenbloom,K.R., Dreszer,T.R., Long,J.C., Malladi,V.S., Sloan,C.A., Raney,B.J., Cline,M.S., Karolchik,D., Barber,G.P., Clawson,H. *et al.* (2012) ENCODE whole-genome data in the UCSC Genome Browser: update 2012. *Nucleic Acids Res.*, **40**, D912–D917.
67. Maher,B. (2012) ENCODE: the human encyclopaedia. *Nature*, **489**, 46–48.
68. Bian,C., Xu,C., Ruan,J., Lee,K.K., Burke,T.L., Tempel,W., Barsyte,D., Li,J., Wu,M., Zhou,B.O. *et al.* (2011) Sgf29 binds histone H3K4me2/3 and is required for SAGA complex recruitment and histone H3 acetylation. *EMBO J.*, **30**, 2829–2842.
69. Schram,A.W., Baas,R., Jansen,P.W., Riss,A., Tora,L., Vermeulen,M. and Timmers,H.T. (2013) A dual role for SAGA-associated factor 29 (SGF29) in ER stress survival by coordination of both histone H3 acetylation and histone H3 lysine-4 trimethylation. *PLoS One*, **8**, e70035.
70. Hung,T., Binda,O., Champagne,K.S., Kuo,A.J., Johnson,K., Chang,H.Y., Simon,M.D., Kutateladze,T.G. and Gozani,O. (2009) ING4 mediates crosstalk between histone H3 K4 trimethylation and H3 acetylation to attenuate cellular transformation. *Mol. Cell*, **33**, 248–256.
71. Protacio,R.U., Li,G., Lowary,P.T. and Widom,J. (2000) Effects of histone tail domains on the rate of transcriptional elongation through a nucleosome. *Mol. Cell Biol.*, **20**, 8866–8878.
72. Walia,H., Chen,H.Y., Sun,J.-M., Holth,L.T. and Davie,J.R. (1998) Histone acetylation is required to maintain the unfolded nucleosome structure associated with transcribing DNA. *J. Biol. Chem.*, **273**, 14516–14522.
73. Khan,D.H., Jahan,S. and Davie,J.R. (2012) Pre-mRNA splicing: role of epigenetics and implications in disease. *Adv. Biol. Regul.*, **52**, 377–388.
74. Spedale,G., Timmers,H.T. and Pijnappel,W.W. (2012) ATAC-king the complexity of SAGA during evolution. *Genes Dev.*, **26**, 527–541.